Electronic Supplementary Material (ESI) for Journal of Materials Chemistry C.

Supporting Information

Molecular Design Opening Two Emission Pathways for High Efficiency and Long Lifetime in Thermally Activated Delayed Fluorescent Organic Light-Emitting Diodes

Ha Lim Lee[1], Kyung Hyung Lee[1], Jun Yeob Lee[1*], Ho Jung Lee[2]

[1]School of Chemical Engineering, Sungkyunkwan University
2066, Seobu-ro, Jangan-gu, Suwon, Gyeonggi, 16419, Korea
[2]LG Chem, Ltd, LG Science Park, 30, Magokjungang 10-ro, Gangseo-gu, Seoul, 07796, Korea

E-mail: leej17@skku.edu,

Keywords: TADF· molecular design· lifetime· efficiency

Experimental

General information

9-phenyl-9H,9'H-3,3'-bicarbazole, 5-phenyl-5,12-dihydroindolo[3,2-a]carbazole were supplied from LG Chem. Ltd. 2,4-dibromo-1-fluorobenzene, bis(pinacolate) diboron were bought from INCO Co. 2-chloro-4,6-diphenyl-1,3,5-triazine, bis(diphenylphosphino)ferrocene]palladium(II) dichloride, tetrakis(triphenylphosphine) palladium(0) were product of P&H Tech Co. Potassium acetate, potassium carbonate, cesium carbonate, 1,4-dioxane, N,N-dimethylformamide (DMF) were supplied from Daejung Chemical & Metal Co.. n-hexane, methylene chloride (MC) , tetrahydrofuran (THF), chloroform were products of Samchun Pure Chemical Co., Ltd.

The Uv-Visible absorption spectra and photoluminescence (PL) emission spectra of BTrzICz and BTrzBCz were measured with UV-vis spectrophotometer (JASCO, V-730) and fluorescence spectrophotometer (PerkinElmer, LS-55), respectively. The photoluminescence quantum yield and transient photoluminescence decay data were measured by using Quantaurus-QY system (Hamamatsu, C11347-11) and Quantaurus-Tau system (Hamamatsu, C11367-31) under N_2 atmosphere. ^{1}H, ^{13}C NMR were measured by using AVNACE III HD (Bruker, 500 MHz) spectrometer for structure analysis. The mass spectroscopy was obtained by using Advion, Expresion^{L} CMS spectrometer with APCI mode and JMS-700 (JEOL) with high resolution fast atom bombardment (FAB) mode. Purity of final products was recorded on high performance liquid chromatography (Younglin Instrument Co.) with mobile phase of tetrahydrofuran:water (7:3). The energy level of HOMO and LUMO was estimated by measurement of cyclic voltammetry (Ivium Tech., Iviumstat) using 0.1 M of tetrabutylammonium perchlorate in acetonitrile solution. For calibration, ferrocene was used.

Synthesis

2,2'-(4-fluoro-1,3-phenylene)bis(4,4,5,5-tetramethyl-1,3,2-dioxaborolane)

2,4-dibromo-1-fluorobenzene (10.00 g, 39.39 mmol), bis(pinacolate) diboron (30.01 g, 118.16 mmol), bis(diphenylphosphino)ferrocene]palladium(II) dichloride (1.73 g, 2.36 mmol) and potassium acetate (23.20 g, 236.32 mmol) were poured into 1,4-dioxane (200 ml). Then the mixture was stirred and refluxed during 12 hours under nitrogen purge. After end of reaction, the mixture was cooled down to room temperature and methylene chloride (300 ml) was added into the mixture. The crude solution was filtered with celite/silica gel. Then filtered organic solution was concentrated by rotary evaporator. The concentrated crude product was purified by column chromatography using a eluent solvent (MC : n-hexane = 1 : 1). A white solid product was obtained as a pure solid (8.30 g, 64% Yield).

^{1}H NMR (500 MHz, $CDCl_3$) : δ 8.21 (d, J=6.50 Hz, 1H), 7.89 (t, J=7.25 Hz, 1H), 7.02 (t, J=9.00 Hz, 1H), 1.36-1.34 (m, 24H)

MS (APCI) m/z : Found 349.23 [(M + H)+]. Calculated For $C_{18}H_{27}B_2FO_4$: 348.03

6,6'-(4-fluoro-1,3-phenylene)bis(2,4-diphenyl-1,3,5-triazine)

2,2'-(4-fluoro-1,3-phenylene)bis(4,4,5,5-tetramethyl-1,3,2-dioxaborolane) (5.00 g, 14.37 mmol) and 2-chloro-4,6-diphenyl-1,3,5-triazine (8.46 g, 31.61 mmol) was dissolved using THF (150 ml) and the solution was poured into 500 ml round-bottom flask. Then the solution was begun to be stirred and heated. 4M solution of potassium carbonate dissolved in deionized water (75 ml) was poured into mixture and tetrakis(triphenylphosphine) palladium(0) (1.66 g, 1.44 mmol) was added into reaction mixture. The reaction was proceeded during 24 hours with nitrogen purge. After 24 hours, the crude product was washed above 10 times with chloroform and filtered. The filtered product showed white powder. (6.52 g, 81% Yield)

^{1}H NMR cannot be measured because of poor solubility.

MS (APCI) m/z : Found 559.17 [(M + H)+]. Calculated For $C_{36}H_{23}FN_6$: 558.61

12-(2,4-bis(4,6-diphenyl-1,3,5-triazin-2-yl)phenyl)-5-phenyl-5,12-dihydroindolo[3,2-a]carbazole (BTrzICz)

6,6'-(4-fluoro-1,3-phenylene)bis(2,4-diphenyl-1,3,5-triazine) (1.00 g, 1.79 mmol), 5-phenyl-5,12-dihydroindolo[3,2-a]carbazole (0.71 g, 2.15 mmol) and cesium carbonate (1.75 g, 5.37 mmol) were added into 100 ml pressure tube. And DMF (10 ml) was added into mixture and the solution was heated and stirred with 150 °C for 3 hours using oil bath. At end of reaction, the mixture was cooled down to room temperature and deionized water was poured into mixture and stirred with 30 minutes. The solution was extracted using MC and extracted organic layer was further concentrated using rotary evaporator. The concentrated crude product was adsorbed into silica gel, and purified by column chromatography using eluent (MC: n-hexane = 1:2). The purified product was sublimated using train sublimation machine with twice. The final product showed bright yellow powder. (0.80 g, 51% Yield)

^{1}H NMR (500 MHz, $CDCl_3$) : δ 9.91 (s, 1H), 9.32 (d, J=8.50 Hz, 1H), 8.87 (d, J=8.50 Hz, 4H), 8.17 (d, J=8.50 Hz, 1H), 8.01 (d, J=7.50 Hz, 1H), 8.10 (d, J=8.50 Hz, 1H), 7.91 (d, J=8.50 Hz, 1H), 7.88 (d, J=8.50 Hz, 4H), 7.65-7.58 (m, 7H), 7.50-7.40 (m, 6H), 7.37 (t, J=7.00 Hz, 1H), 7.32 (t, J=7.75 Hz, 1H), 7.27 (t, J=7.75 Hz, 4H), 7.18-7.10 (m, 3H), 6.82 (t, J=7.00 Hz, 1H), 6.45 (d, J=8.00 Hz, 1H), ^{13}C NMR (125 MHz, $CDCl_3$) : δ 172.2, 172.0, 171.1, 170.8, 143.4, 142.1, 141.6, 140.6, 137.9, 137.8, 137.4, 137.1, 136.3, 135.7, 133.2, 133.0, 132.5, 132.4, 131.9, 129.9, 129.4, 129.1, 129.0, 128.4, 128.2, 128.0, 125.1, 124.7, 124.5, 123.0, 121.8, 120.5, 1119.9, 129.3, 118.5, 118.0, 110.4, 109.4, 108.0, 103.6

MS (HR-FAB) m/z : Found 871.3306 [(M + H)+]. Calculated For $C_{60}H_{38}N_8$: 871.3298

T_g : 171.1 °C, T_d : 505.1 °C (Figure S4, S5)

9-(2,4-bis(4,6-diphenyl-1,3,5-triazin-2-yl)phenyl)-9'-phenyl-9H,9'H-3,3'-bicarbazole (BTrzBCz)

The synthetic method was almost same except starting material, which was 9-phenyl-9H,9'H-3,3'-bicarbazole (0.88 g, 2.15 mmol). The final product showed yellow powder. (0.95 g, Yield 56%)

^{1}H NMR (500 MHz, $CDCl_3$) : δ 10.01 (s, 1H), 9.19 (d, J=8.00 Hz, 1H), 8.87 (d, J=8.00 Hz, 4H), 8.41 (s, 1H), 8.37 (s, 1H), 8.21 (d, J=7.50 Hz, 1H), 8.14-8.11 (m, 5H), 7.97 (d, J=8.00 Hz, 1H), 7.74 (d, J=8.50 Hz, 2H), 7.65-7.59 (m, 10H), 7.50-7.40 (m, 7H), 7.35-7.25 (m, 8H),

^{13}C NMR (125 MHz, $CDCl_3$) : δ 172.2, 172.0, 171.7, 170.8, 142.1, 141.5, 141.0, 140.7, 140.2, 138.0, 136.9, 136.4, 136.2, 135.7, 134.6, 134.4, 134.0, 133.0, 132.9, 132.6, 131.1, 130.1, 129.3, 129.1, 129.0, 128.6, 127.6, 127.3, 126.4, 126.2, 126.2, 126.0, 124.6, 124.2, 124.1, 123.8, 120.6, 120.6, 120.2, 120.1, 119.1, 119.1, 110.2, 110.1, 109.9

MS (HR-FAB) m/z : Found 947.3611 [(M + H)+]. Calculated For $C_{66}H_{42}N_8$: 947.3611

T_g : 170.1 °C, T_d : 556.4 °C (Figure S4, S5)

Device Fabrication

All of substrates were washed before organic deposition using chloroform, isopropyl alcohol and deionized water. The chemical deposition was performed under 5.0 x 10^{-7} torr. The device structure was summarized as below.

ITO (50 nm)/DNTPD (60 nm)/BPBPA (20 nm)/PCZAC (10 nm)/CzTrz:Emitter (30 nm, 3~20 wt%)/DBFTrz (5 nm)/ZADN (30 nm)/LiF (1.5 nm)/Al (200 nm)

where DNTPD is N,N′-diphenyl-N,N′-bis-[4-(phenyl-m-tolyl-amino)-phenyl]-biphenyl-4,4′-diamine, BPBPA is N4,N4,N4′,N4′-tetra([1,1′-biphenyl]-4-yl)-[1,1′-biphenyl]-4,4′-diamine, PCZAC is 9,9-dimethyl-10-(9-phenyl-9H-carbazol-3-yl)-9,10-dihydroacridine, DBFTrz is

2,8-bis(4,6-diphenyl-1,3,5-triazin-2-yl)dibenzo[b,d]furan and ZADN is 2-[4-(9,10-di-naphthalen-2-yl-anthracene-2-yl)-phenyl]-1-phenyl-1H-benzimidazole. CzTrz is host material, 9-(3'-(4,6-diphenyl-1,3,5-triazin-2-yl)-[1,1'-biphenyl]-3-yl)-9H-carbazole.

Each materials' role was already reported in our previous work. In emissive layer, BTrzICz and BTrzBCz was doped into CzTrz host with 3, 5, 10 and 20 wt% doping concentration. 4CzIPN device was fabricated only with 20 wt% doping concentration.

List of Table

Table S1. Spin-orbit coupling value of BTrzICz and BTrzBCz based on vertical absorption calculation.

Emitter	$S_0 \rightarrow S_1$ (eV)	$S_0 \rightarrow T_1$ (eV)	$S_0 \rightarrow T_2$ (eV)	$\langle S_1\|H_{SO}\|T_1\rangle$ (cm^{-1})	$\langle S_1\|H_{SO}\|T_2\rangle$ (cm^{-1})
BTrzICz	**3.13**	**2.98**	**3.25**	**0.09**	**0.06**
BTrzBCz	**3.14**	**2.97**	**3.41**	**0.08**	**0.07**

Table S2. Vertical emission **c**alculation results of BTrzICz and BTrzBCz at the lowest singlet and triplet excited state

	Transition Involved States (Characteristic)	**Transition Probability**	**Oscillator Strength (f)**
BTrzICz ($S_1 \rightarrow S_0$)	HONTO-1 → LUNTO (Mix)	7.3%	0.0053
	HONTO → LUNTO (CT)	81.6%	
	HONTO → LUNTO+2 (CT)	3.5%	
BTrzICz ($T_1 \rightarrow S_0$)	HONTO-9 → LUNTO (LE)	3.9%	0.0000
	HONTO-7 → LUNTO (CT)	2.3%	
	HONTO-5 → LUNTO (Mix)	9.6%	
	HONTO-2 → LUNTO (LE)	9.2%	
	HONTO-1 → LUNTO (LE)	19.3%	
	HONTO → LUNTO (Mix)	39.0%	
BTrzBCz ($S_1 \rightarrow S_0$)	HONTO-2 → LUNTO (Mix)	2.3%	0.0188
	HONTO-1 → LUNTO (CT)	10.7%	
	HONTO → LUNTO (CT)	76.9%	
	HONTO → LUNTO+2 (CT)	3.2%	
BTrzBCz ($T_1 \rightarrow S_0$)	HONTO-11 → LUNTO (LE)	2.3%	0.0000
	HONTO-10 → LUNTO (CT)	4.0%	
	HONTO-9 → LUNTO (CT)	2.6%	
	HONTO-5 → LUNTO (LE)	2.9%	
	HONTO-4 → LUNTO (Mix)	2.6%	
	HONTO-2 → LUNTO (Mix)	5.8%	
	HONTO-1 → LUNTO (LE)	23.0%	
	HONTO → LUNTO (Mix)	41.1%	

Table S3. Device performance of BTrzICz and BTrzBCz at 3,000 cd/m^2

	V_d (V)	EL spectrum (nm)	CIE	QE(%)	
				[3,000 cd/m^2]	[Max]
CzTrz:BTrzICz (3 wt%)	7.0	515	(0.27, 0.53)	17.9	18.8
CzTrz:BTrzICz (5 wt%)	6.7	515	(0.27, 0.54)	19.8	20.6
CzTrz:BTrzICz (10 wt%)	6.5	521	(0.29, 0.56)	20.1	20.7
CzTrz:BTrzICz (20 wt%)	6.1	523	(0.30, 0.57)	20.5	20.7
CzTrz:BTrzBCz (3 wt%)	7.1	515	(0.27, 0.54)	14.5	17.6
CzTrz:BTrzBCz (5 wt%)	7.0	515	(0.28, 0.55)	16.9	20.2
CzTrz:BTrzBCz (10 wt%)	6.7	521	(0.30, 0.57)	18.7	20.7
CzTrz:BTrzBCz (20 wt%)	6.4	522	(0.31, 0.58)	18.9	20.5

Table S4. Comparison device data of BTrzICz, BTrzBCz and 4CzIPN

	V_d (V)	QE(%)			
		[100 cd/m^2]	[1,000 cd/m^2]	[10,000 cd/m^2]	[Max]
CzTrz:BTrzICz (20 wt%)	7.1	16.7	20.6	18.9	20.7
CzTrz:BTrzBCz (20 wt%)	7.5	18.9	20.2	15.5	20.5
CzTrz:4CzIPN (20 wt%)	8.8	13.1	13.5	12.0	13.5

*Vd= Driving voltage at 10,000 cd/m2

Table S5. Comparison lifetime data of the state of the art devices

Emitter	Device Structure	CIE	Max EQE	Lifetime	Ref
4CzIPN	ITO/HAT-CN (10 nm)/Tris-PCz (30 nm)/mCBP:4CzIPN (30 nm: 15 wt%)/Liq (1 or 2 or 3 nm)/T2T (10 nm)/BPy-TP2 (40 nm)/LiF (0.8 nm)/Al (100 nm)	(0.34, 0.59)	7.5%	485 h @LT90 At 1,000 cd/m^2	**1**
		(0.34, 0.59)	7.3%	630 h @LT90 At 1,000 cd/m^2	
		(0.34, 0.59)	4.7%	1,115 h @LT90 At 1,000 cd/m^2	
	ITO/HAT-CN (10 nm)/Tris-PCz (30 nm)/mCBP:4CzIPN (30 nm: 15 wt%)/T2T (10 nm)/Liq (1 or 2 or 3 nm)/BPy-TP2 (40 nm)/LiF (0.8 nm)/Al (100 nm)	(0.34, 0.59)	15.9%	290 h @LT90 At 1,000 cd/m^2	
		(0.34, 0.59)	15.8%	140 h @LT90 At 1,000 cd/m^2	
		(0.34, 0.59)	14.0%	30 h @LT90 At 1,000 cd/m^2	
	ITO/HAT-CN (10 nm)/Tris-PCz (30 nm)/mCBP:4CzIPN (30 nm: 15 wt%)/Liq (3 nm)/T2T (10 nm)/Liq (1 or 2 or 3 nm)/BPy-TP2 (40 nm)/LiF (0.8 nm)/Al (100 nm)	(0.34, 0.59)	4.4%	1,130 h @LT90 At 1,000 cd/m^2	
		(0.34, 0.59)	4.4%	1,380 h @LT90 At 1,000 cd/m^2	
		(0.34, 0.59)	4.2%	1,045 h @LT90 At 1,000 cd/m^2	
	ITO (120 nm)/PEDOT:PSS (60 nm)/TAPC (20 nm)/mCP (10 nm)/DBTTP1:4CzIPN (25 nm)/TSPO1 (5 nm)/TPBi (30 nm)/LiF (1 nm)/Al (200 nm)	-	18.7%	~250 h @LT80 At 1,000 cd/m^2	**2**
	ITO (120 nm)/PEDOT:PSS (60 nm)/TAPC (20 nm)/mCP (10 nm)/DBTTP2:4CzIPN (25 nm)/TSPO1 (5 nm)/TPBi (30 nm)/LiF (1 nm)/Al (200 nm)	-	20.0%	~90 h @LT80 At 1,000 cd/m^2	
	ITO (50 nm)/DNTPD (60 nm)/BPBPA (20 nm)/PCzAc (10 nm)/CzTrz: 4CzIPN (30 nm: 20 wt%)/DBFTrz (5 nm)/ZADN (30 nm)/LiF (1.5 nm)/Al (200 nm)	(0.34, 0.60)	13.5%	32 h @LT95 At 1,000 cd/m^2	**This Work**
BTrzICz	ITO (50 nm)/DNTPD (60 nm)/BPBPA (20 nm)/PCzAc (10 nm)/CzTrz: BTrzICz (30 nm: 20 wt%)/DBFTrz (5 nm)/ZADN (30 nm)/LiF (1.5 nm)/Al (200 nm)	(0.30, 0.57)	20.7%	86 h @LT95 At 1,000 cd/m^2	
BTrzBCz	ITO (50 nm)/DNTPD (60 nm)/BPBPA (20 nm)/PCzAc (10 nm)/CzTrz: BTrzBCz (30 nm: 20 wt%)/DBFTrz (5 nm)/ZADN (30 nm)/LiF (1.5 nm)/Al (200 nm)	(0.31, 0.58)	20.5%	64 h @LT95 At 1,000 cd/m^2	

List of Figure

(a)

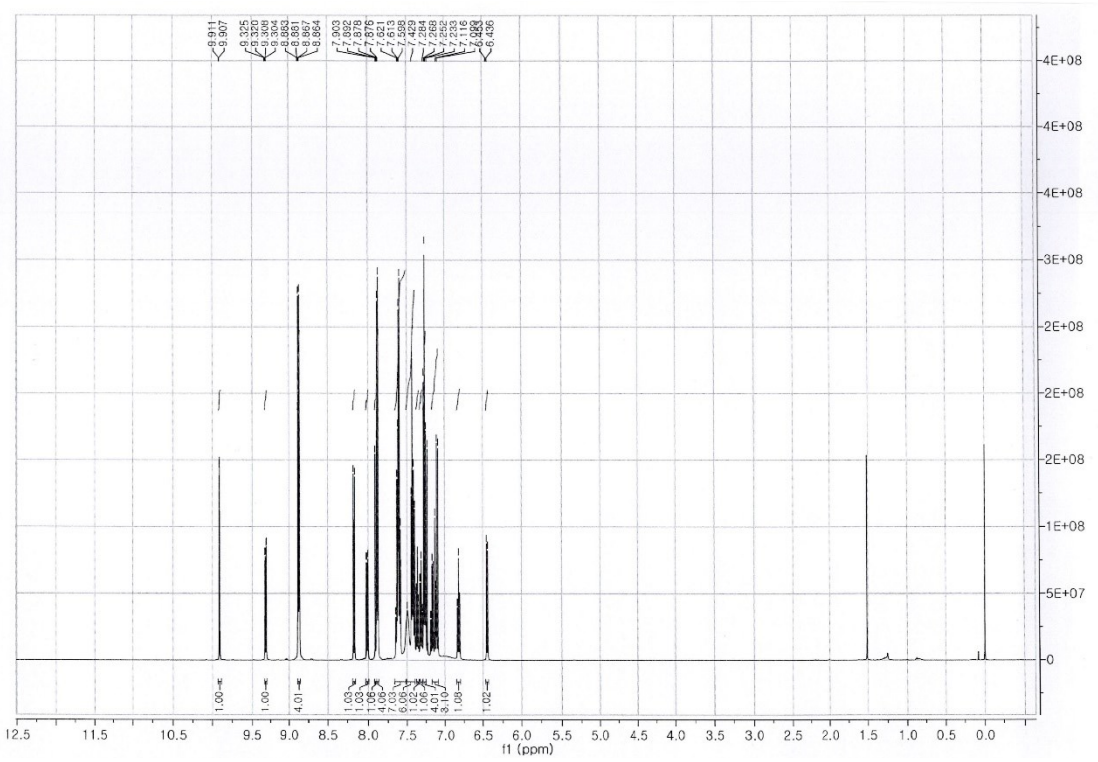
9.911
9.907
9.325
9.320
9.308
9.304
8.881
8.861
8.867
8.864
7.903
7.892
7.878
7.875
7.871
7.513
7.508
7.489
7.484
7.268
7.252
7.213
7.116
6.436
1.00
1.00
4.01
1.03
1.03
1.06
4.05
7.03
6.06
1.02
1.06
4.01
3.10
1.08
1.02
4E+08
4E+08
4E+08
3E+08
2E+08
2E+08
2E+08
1E+08
5E+07
0
12.5
11.5
10.5
9.5
9.0
8.5
8.0
7.5
7.0
6.5
6.0
5.5
5.0
4.5
4.0
3.5
3.0
2.5
2.0
1.5
1.0
0.5
0.0
f1 (ppm)

(b)

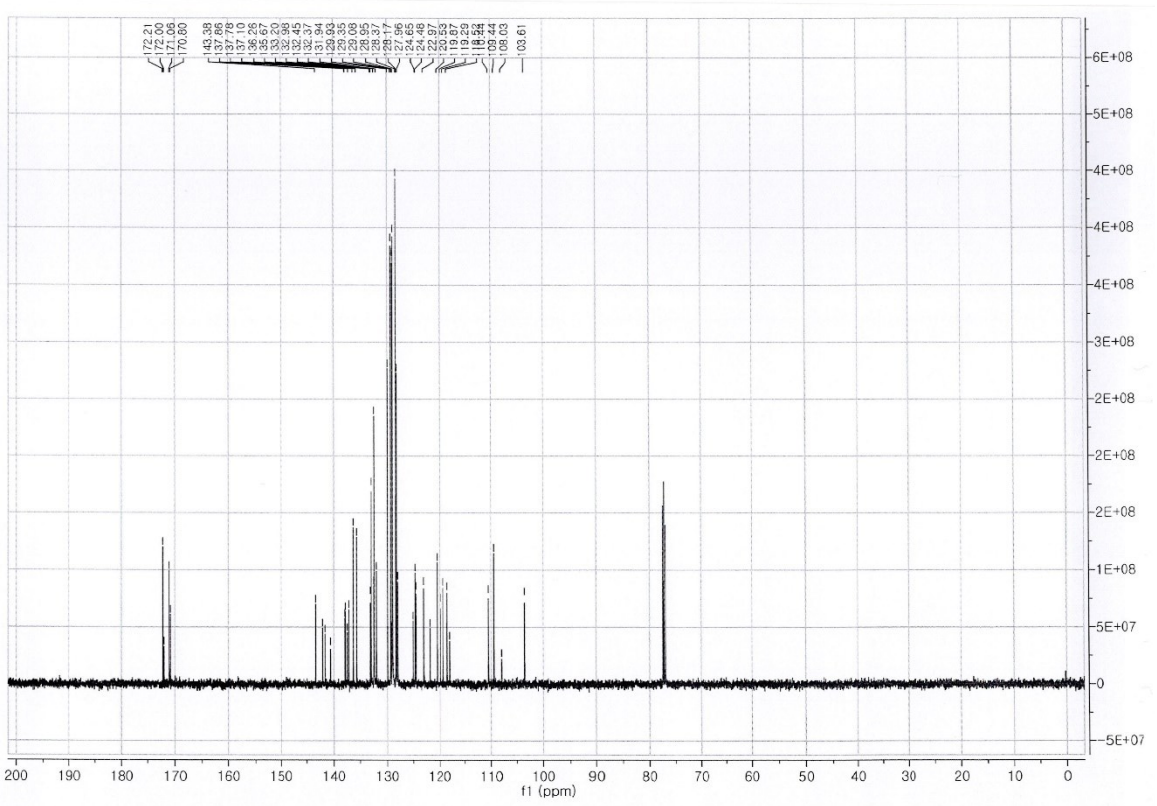
172.21
172.00
171.06
170.80
143.38
137.86
137.78
137.10
136.26
135.67
135.20
132.99
132.45
132.37
131.84
129.93
129.35
129.09
128.95
128.37
128.17
127.96
124.65
124.48
122.97
120.53
119.87
119.29
118.94
118.62
109.44
108.03
103.61
6E+08
5E+08
4E+08
4E+08
4E+08
3E+08
2E+08
2E+08
2E+08
1E+08
5E+07
0
-5E+07
200 190 180 170 160 150 140 130 120 110 100 90 80 70 60 50 40 30 20 10 0
f1 (ppm)

(c)

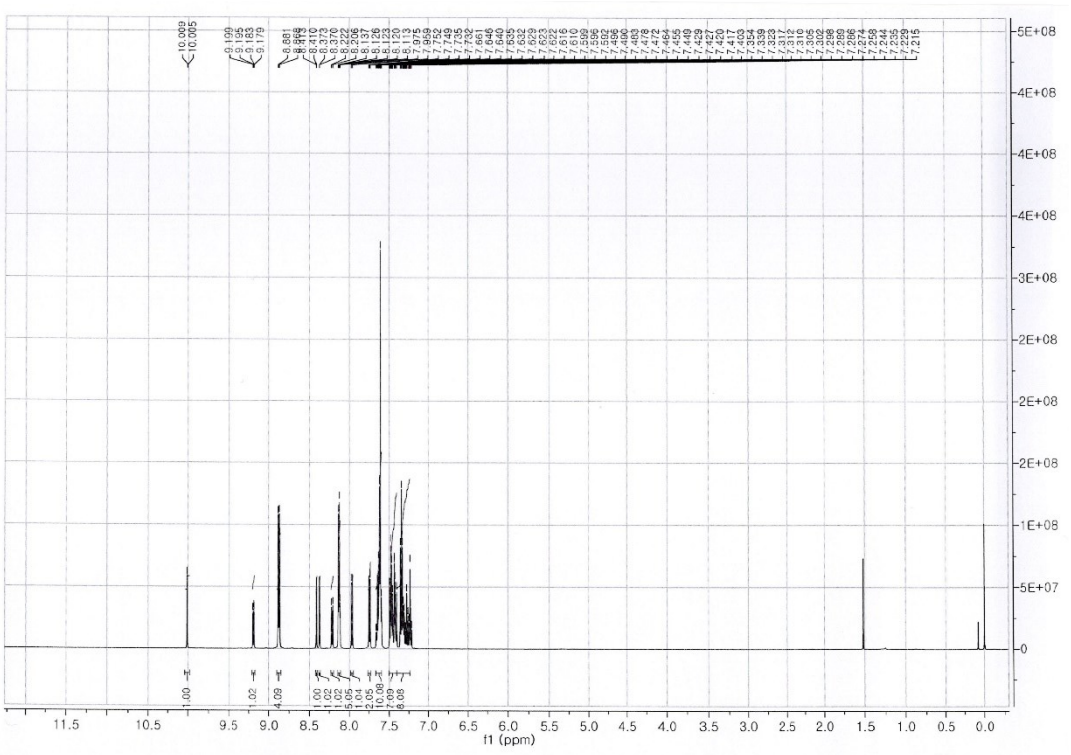
10.009
10.005
9.190
9.185
9.179
6.881
8.410
8.373
8.222
8.206
8.137
8.123
8.120
7.959
7.752
7.749
7.732
7.661
7.640
7.635
7.632
7.629
7.623
7.622
7.616
7.610
7.596
7.592
7.486
7.483
7.478
7.472
7.464
7.455
7.449
7.429
7.427
7.420
7.417
7.354
7.339
7.323
7.312
7.310
7.302
7.298
7.288
7.274
7.258
7.244
7.229
7.215
1.00
1.02
4.09
1.00
1.02
1.02
1.05
1.04
2.05
10.08
7.68
8.09
5E+08
4E+08
4E+08
4E+08
3E+08
2E+08
2E+08
2E+08
1E+08
5E+07
0
11.5
10.5
9.5
9.0
8.5
8.0
7.5
7.0
6.5
6.0
5.5
5.0
4.5
4.0
3.5
3.0
2.5
2.0
1.5
1.0
0.5
0.0
f1 (ppm)

(d)

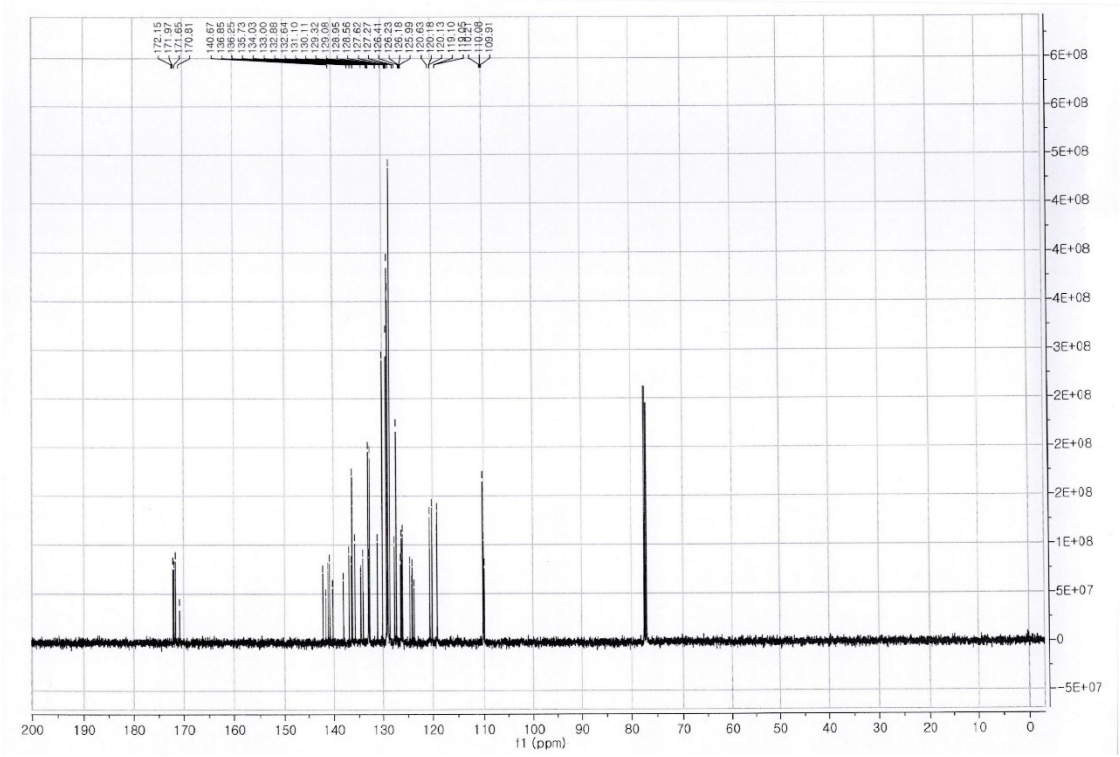

Figure S1. ^{1}H, ^{13}C NMR spectra of (a,b) BTrzICz and (c,d) BTrzBCz

(a)

```
Note : m-NBA
Inlet : Direct                          Ion Mode : FAB+
RT : 0.54 min                           Scan#: (3,42)
Elements : C 100/0, H 100/0, N 10/0
Mass Tolerance      : 20ppm, 5mmu if m/z < 250, 10mmu if m/z > 500
Unsaturation (U.S.) : -0.5 - 50.0

Observed m/z Int%   Err[ppm / mmu]    U.S.  Composition
  871.3306   100.0     -6.8 /  -5.9   48.5  C 69 H 43
                       +7.7 /  +6.7   49.0  C 68 H 41 N
                       +0.9 /  +0.8   45.5  C 60 H 39 N 8
```

(b)

```
Note : m-NBA
Inlet : Direct                          Ion Mode : FAB+
RT : 0.80 min                           Scan#: (18,48)
Elements : C 100/0, H 100/0, N 10/0
Mass Tolerance      : 20ppm, 5mmu if m/z < 250, 10mmu if m/z > 500
Unsaturation (U.S.) : -0.5 - 50.0

Observed m/z Int%   Err[ppm / mmu]    U.S.  Composition
  947.3611   100.0     +0.0 /  +0.0   49.5  C 66 H 43 N 8
```

Figure S2. High resolution mass spectra of (a) BTrzICz and (b) BTrzBCz

(a)

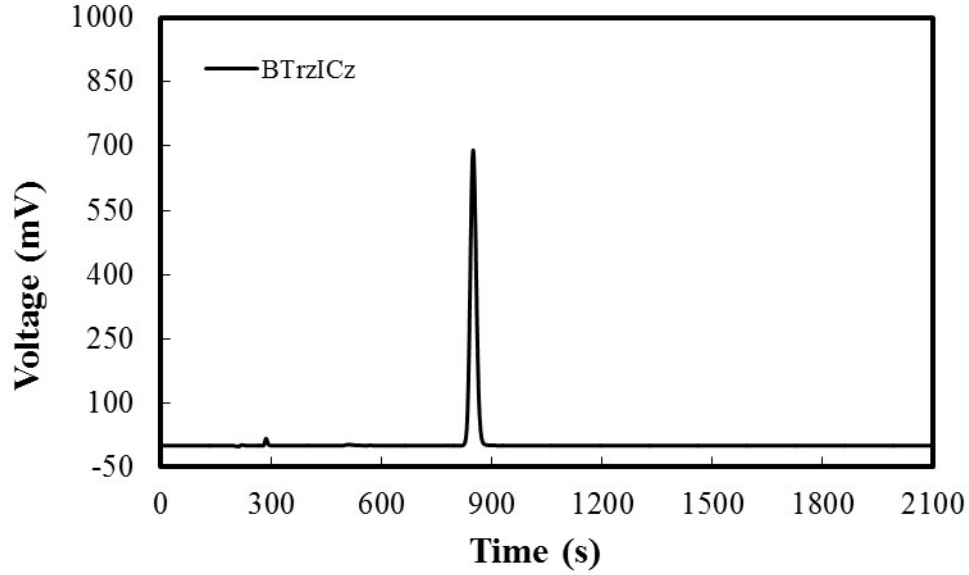

(b)

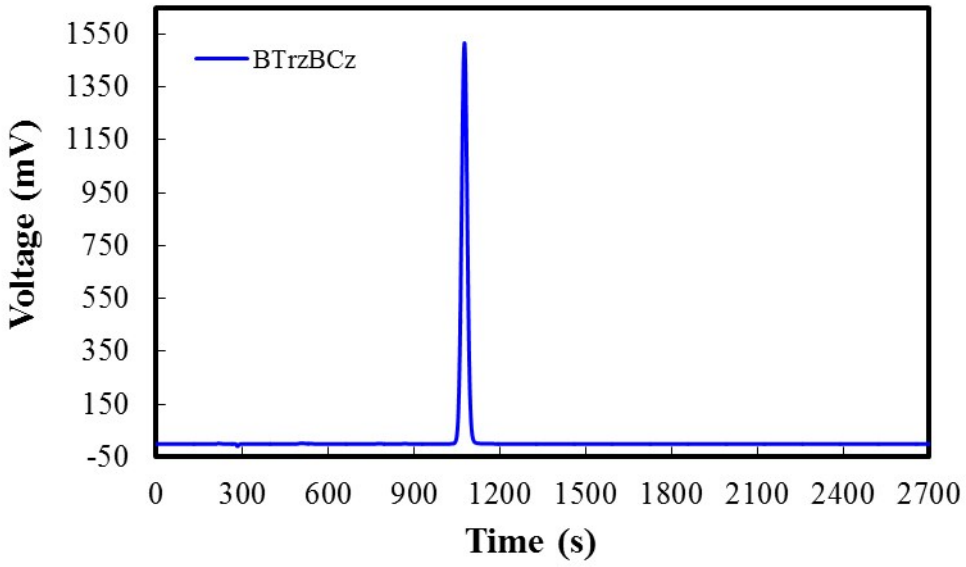

Figure S3. High performance liquid chromatography data of (a) BTrzICz and (b) BTrzBCz

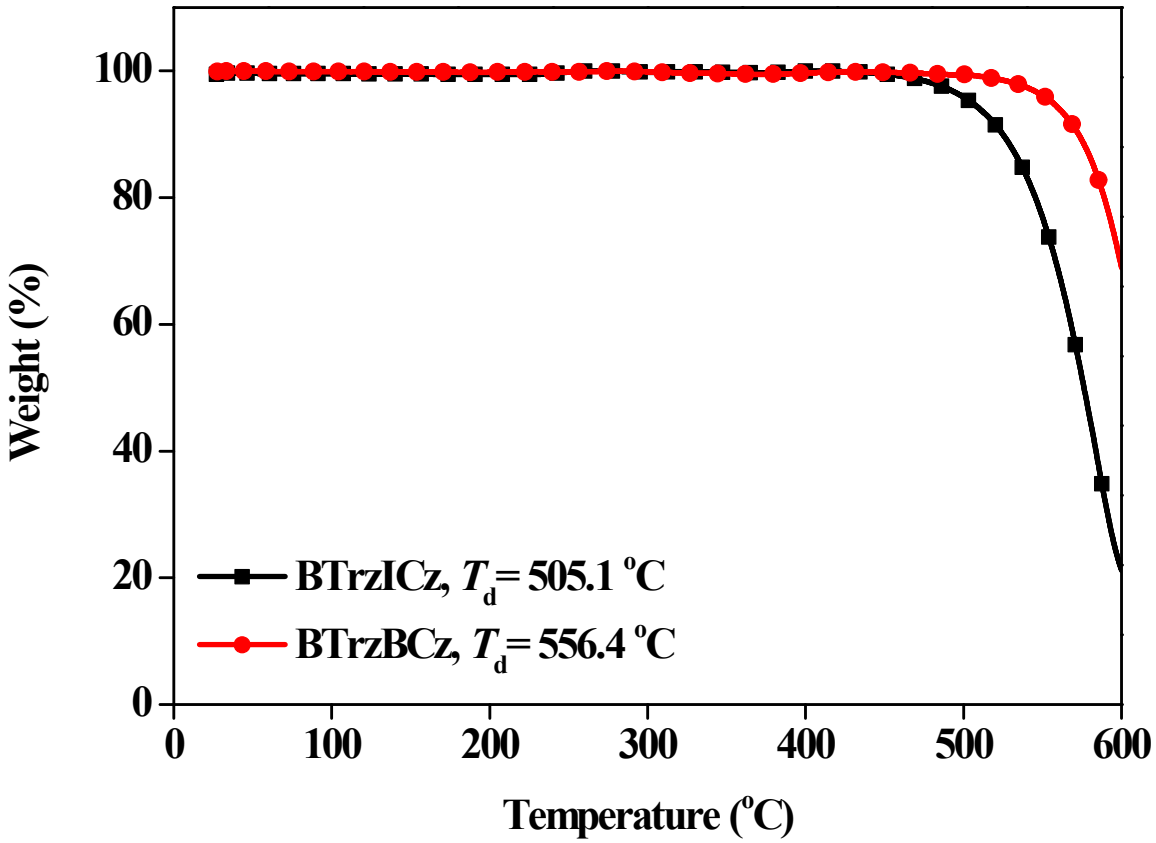

Figure S4. Thermogravimetric analysis data of TADF emitters

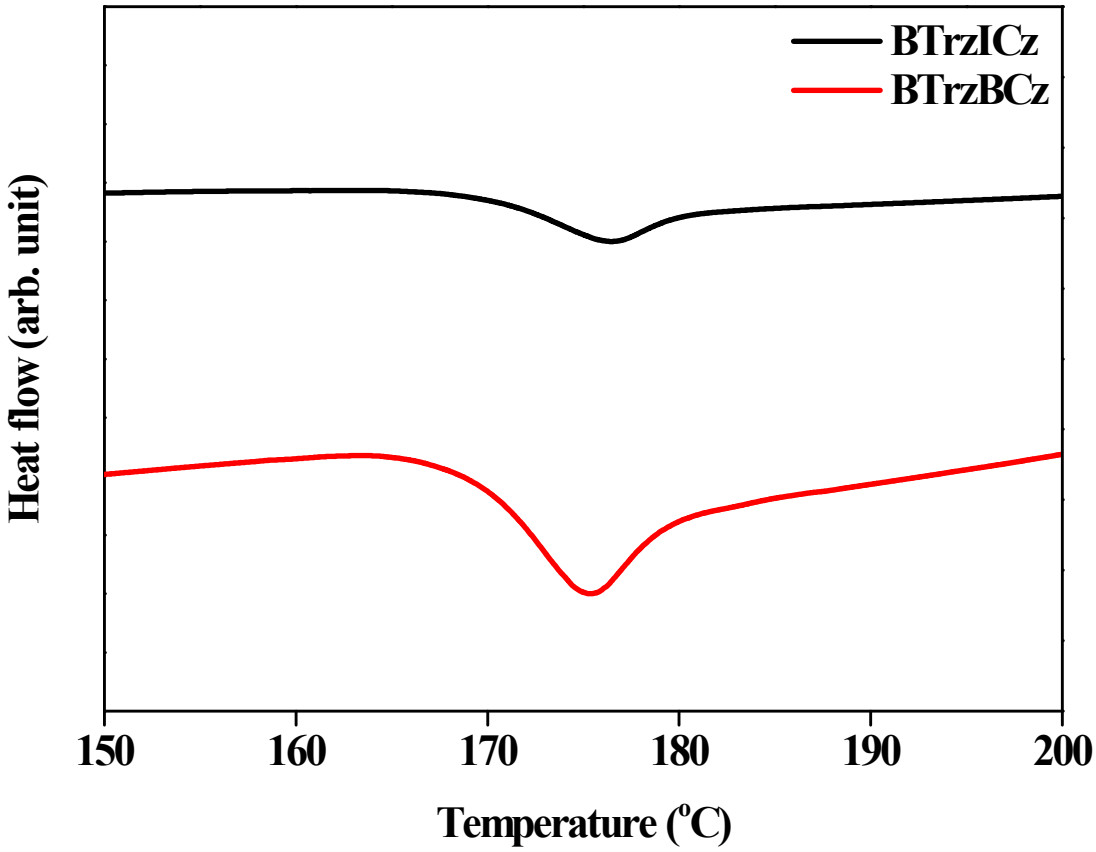

Figure S5. Differential scanning calorimetry data of TADF emitters

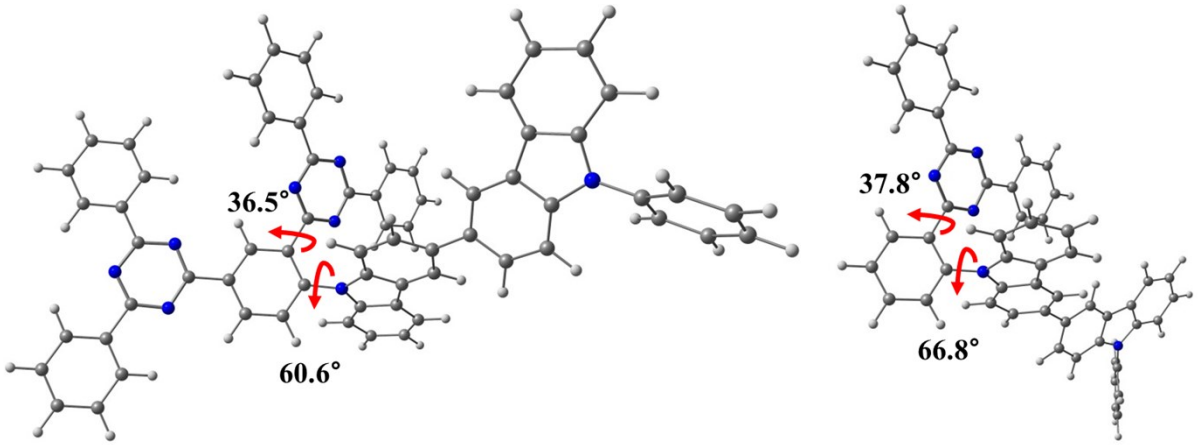

Figure S6. Ground state optimized structures of BTrzBCz and oBCzTrz

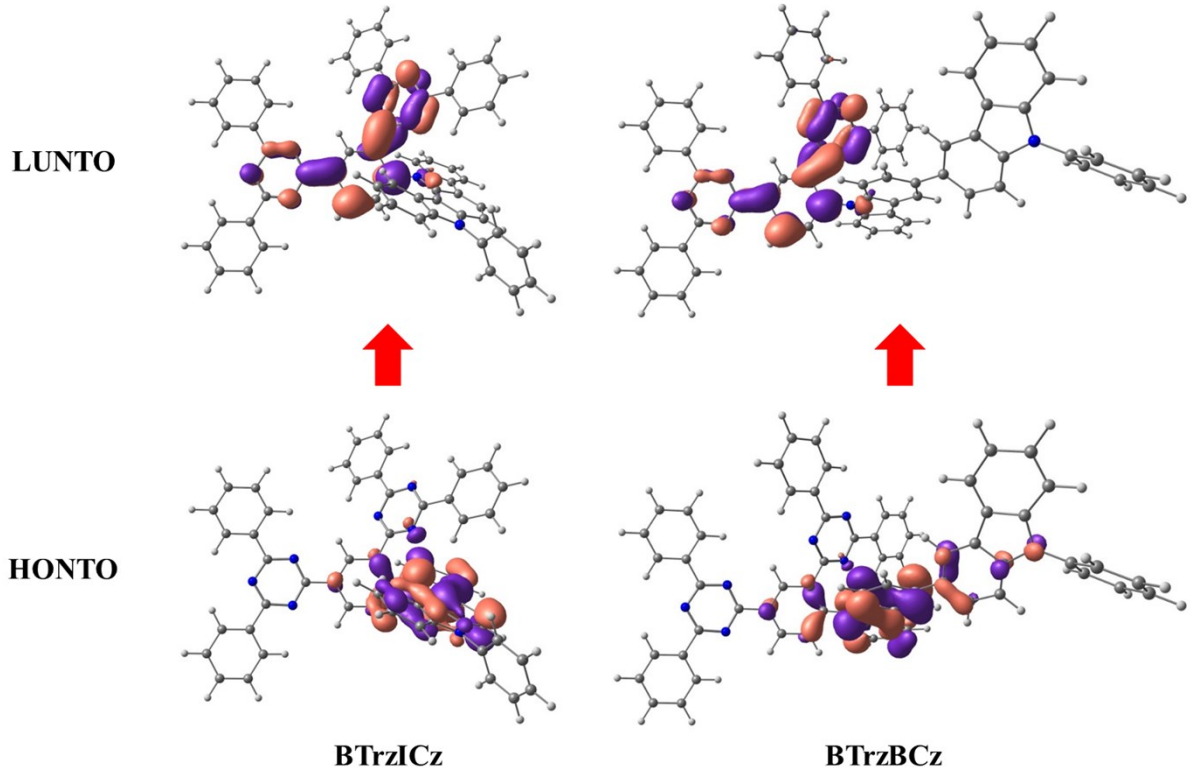

Figure S7. Vertical absorption calculation results of BTrzICz and BTrzBCz

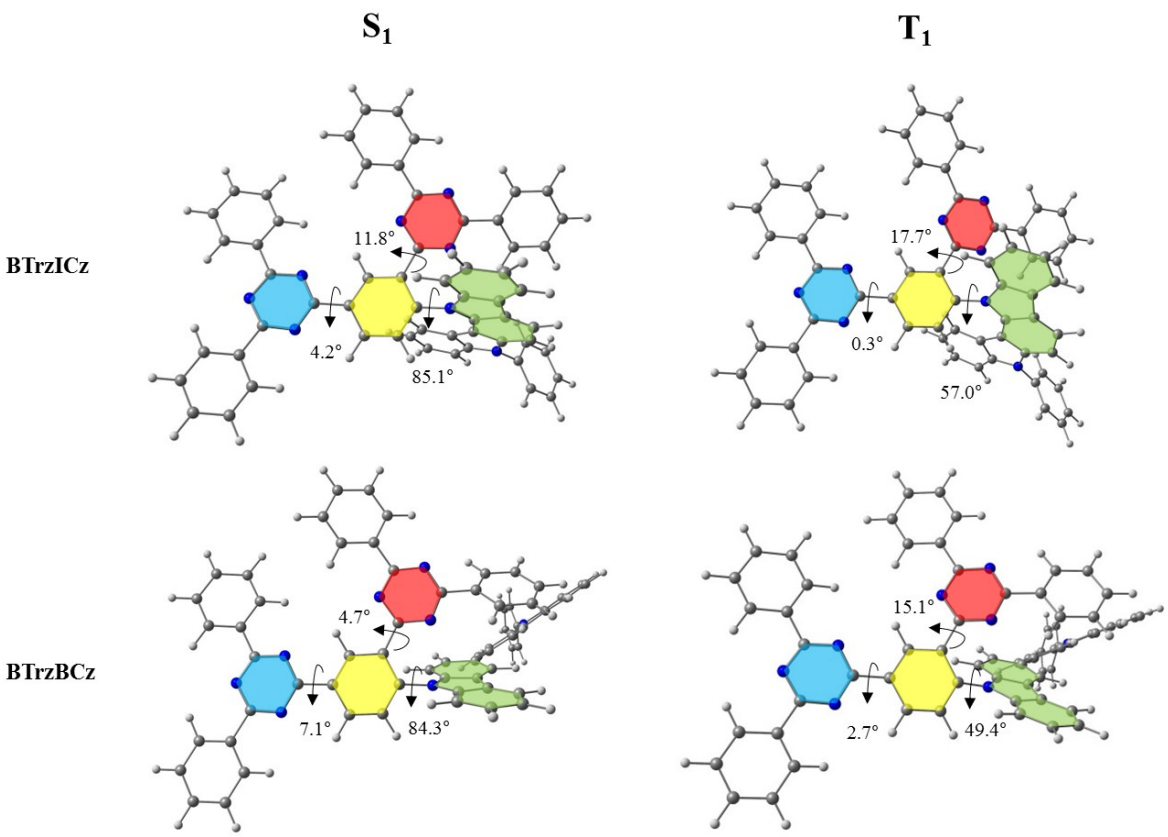

Figure S8. Excited state optimized structures of BTrzICz and BTrzBCz

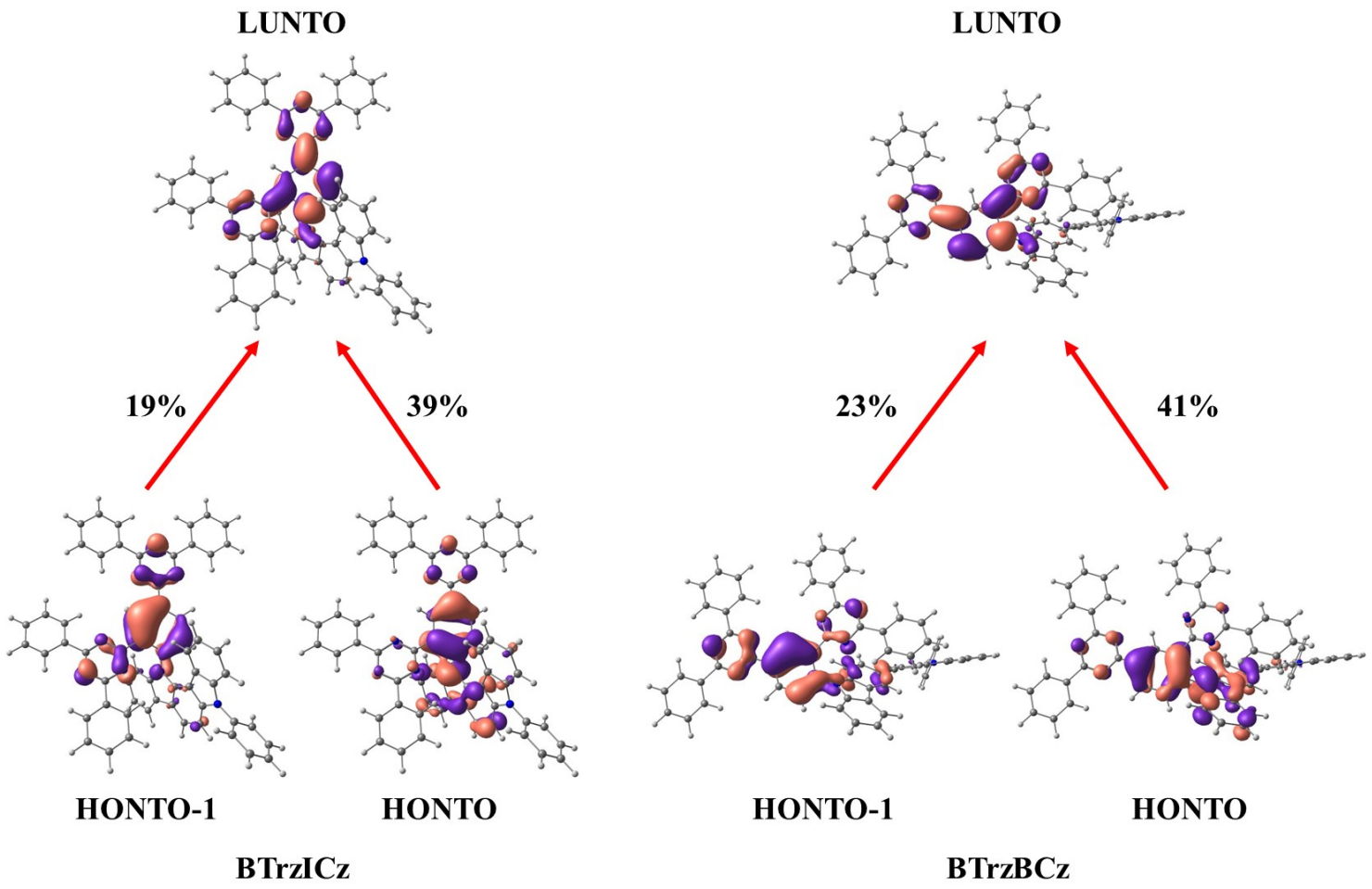

Figure S9. NTO calculation of BTrzICz and BTrzBCz in triplet excited state

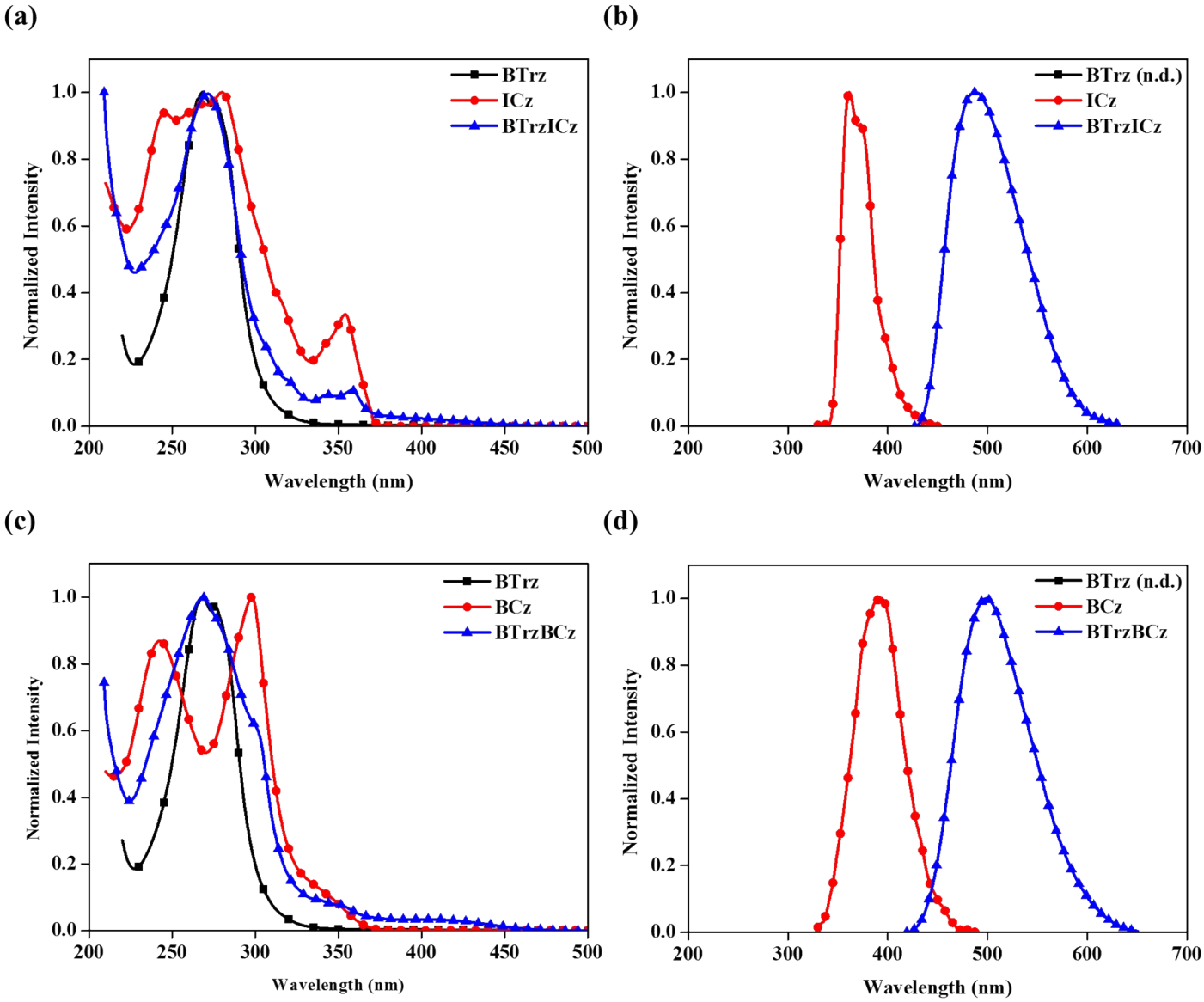

Figure S10. Comparison UV-Vis absorption and PL emission spectra of (a, b) BTrzICz and (c, d) BTrzBCz with individual donor and acceptor moiety.

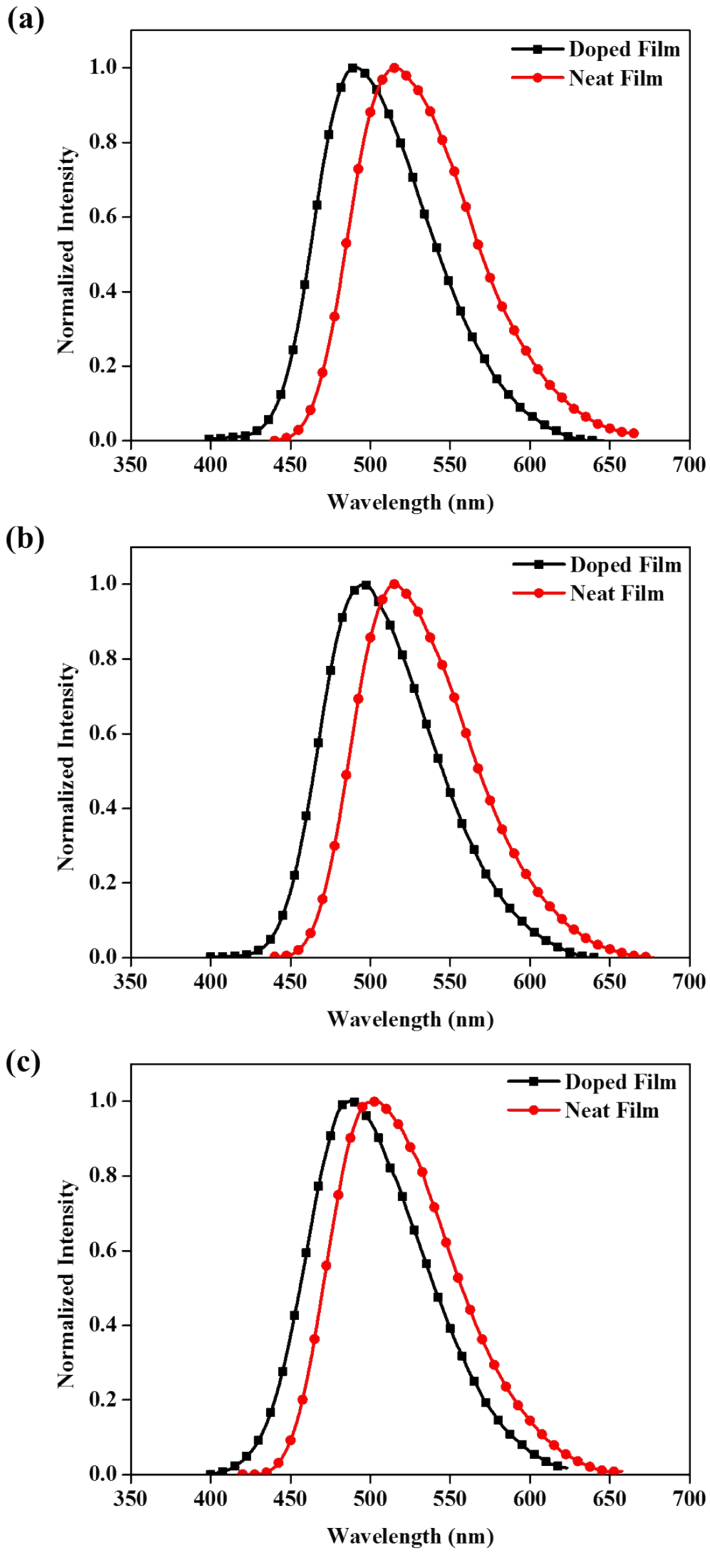

Figure S11. Comparison fluorescence emission spectra of doped film and neat film (a) BTrzICz, (b) BTrzBCz and (c) oBCzTrz

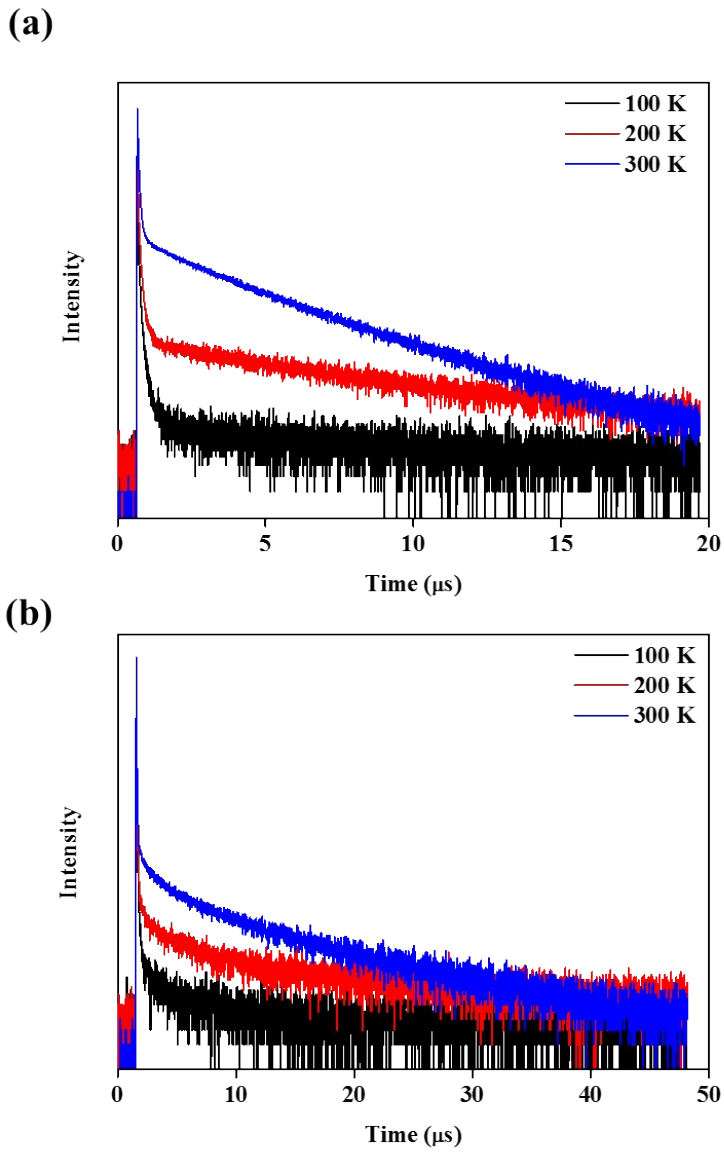

Figure S12. Temperature dependent transient PL curves of (a) BTrzICz and (b) BTrzBCz

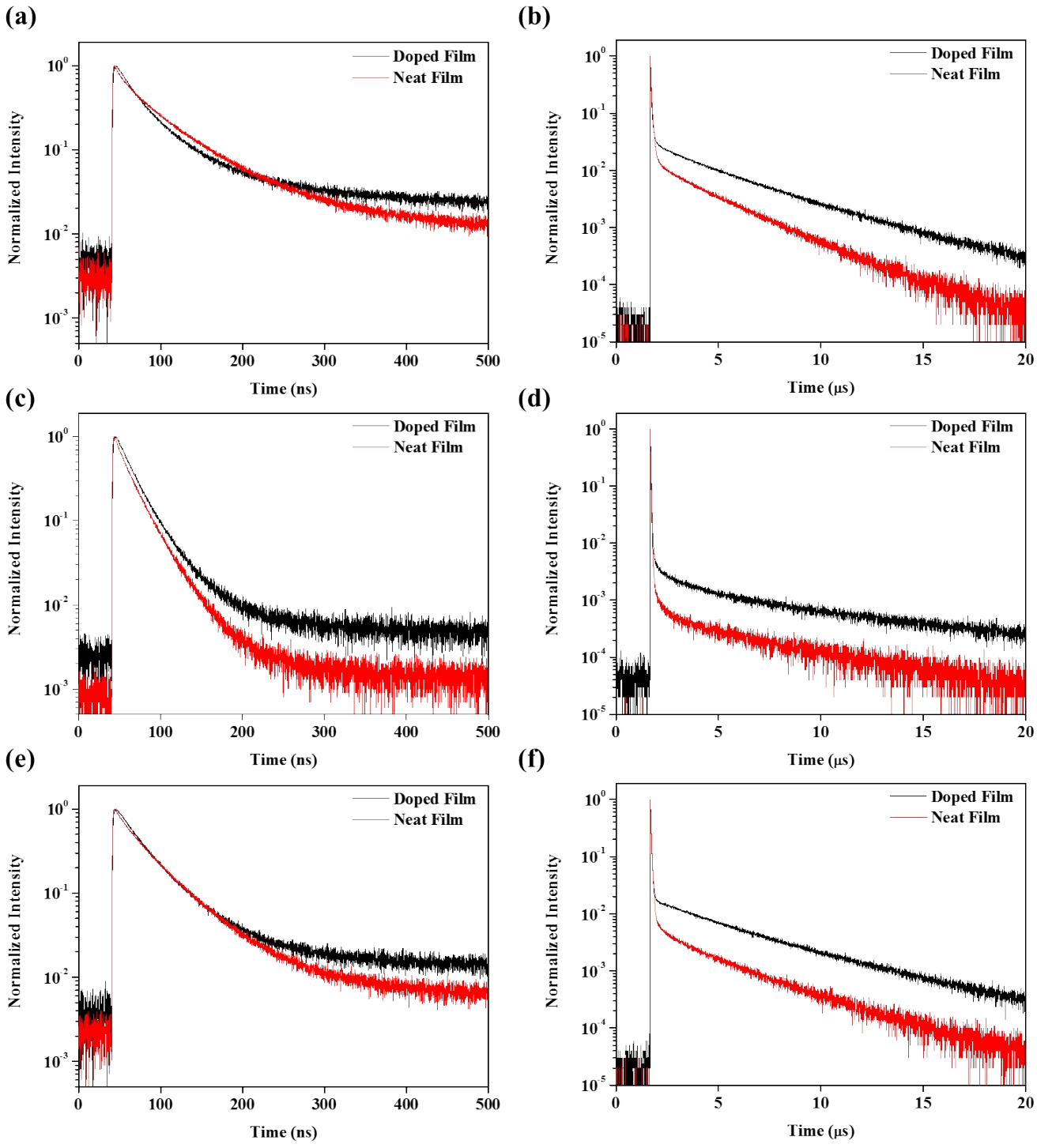

Figure S13. Comparison transient PL curves of prompt component and delay component of (a, B) BTrzICz, (c, d) BTrzBCz, and (e, f) oBCzTrz

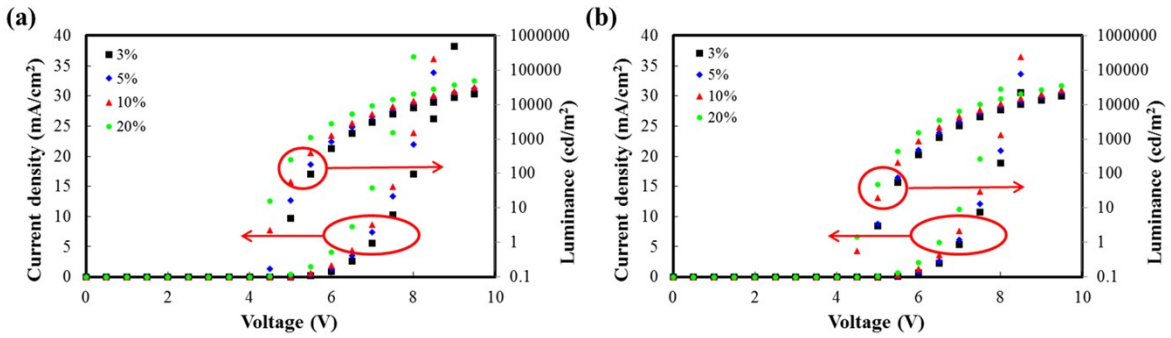

Figure S14. The current density (J)–voltage (V)–luminance (L) curves of (a) BTrzICz and (b) BTrzBCz according to doping concentration

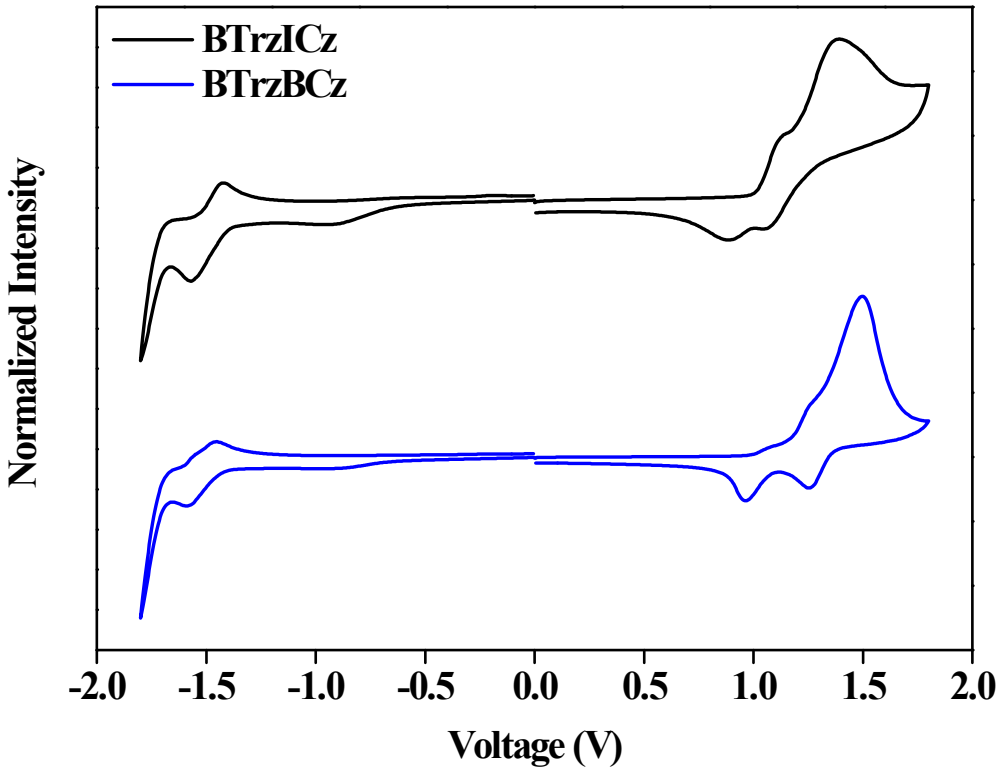

Figure S15. The cyclic voltammetry data of two TADF emitters.

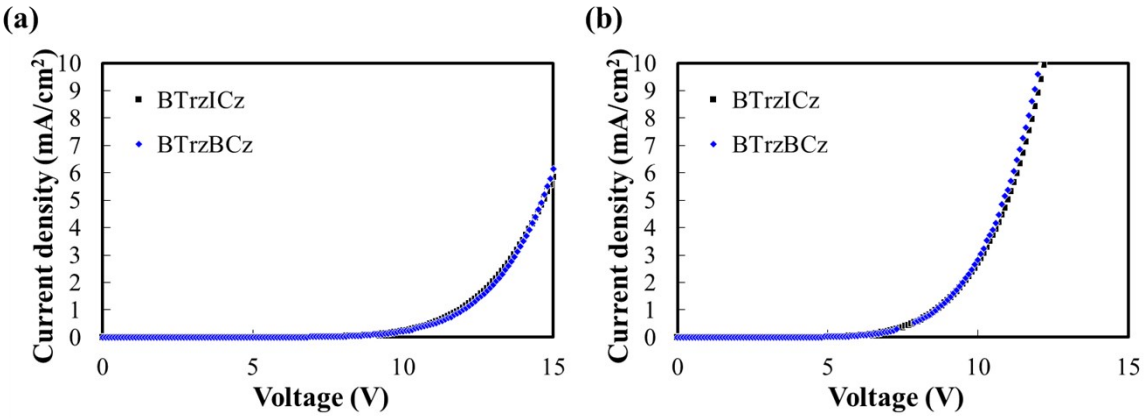

Figure S16. (a) hole and (b) electron single charge devices of the BTrzICz and BTrzBCz (20 wt%)

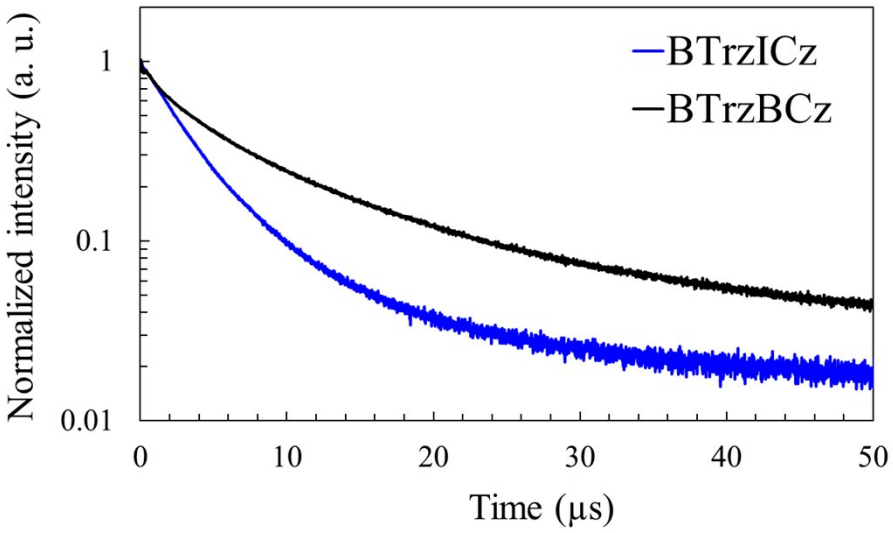

Figure S17. The transient EL data of the BTrzICz and BTrzBCz (20%) devices.

(a)

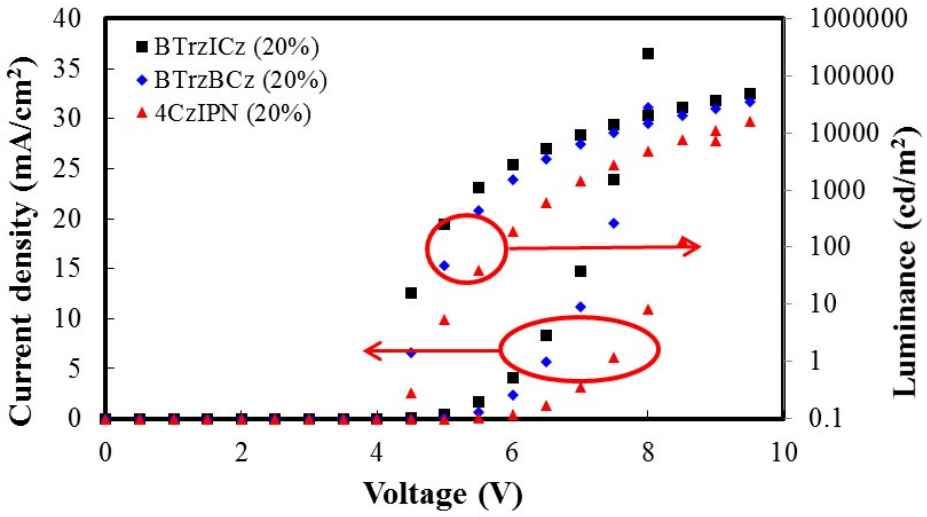
BTrzICz (20%)
BTrzBCz (20%)
4CzIPN (20%)
Current density (mA/cm²)
Luminance (cd/m²)
Voltage (V)
0
5
10
15
20
25
30
35
40
0.1
1
10
100
1000
10000
100000
1000000
0
2
4
6
8
10

(b)

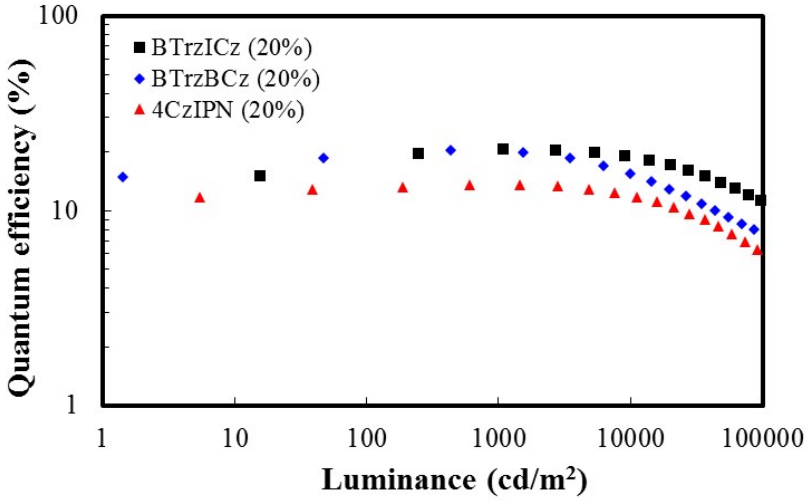
BTrzICz (20%)
BTrzBCz (20%)
4CzIPN (20%)
Quantum efficiency (%)
Luminance (cd/m²)
1
10
100
1
10
100
1000
10000
100000

(c)

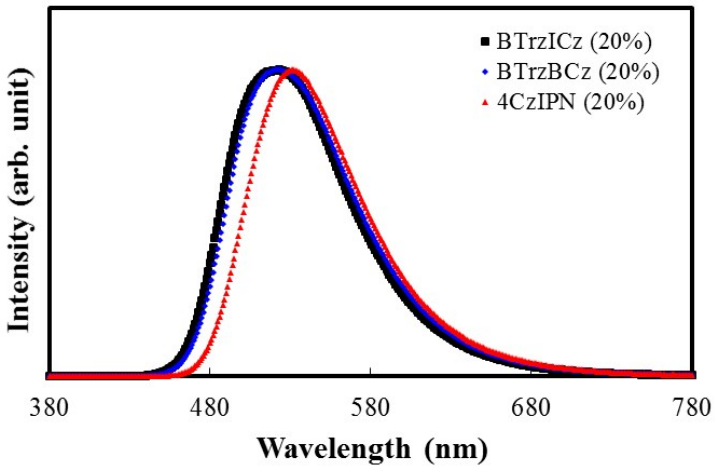

Figure S18. (a) J-V-L curves, (b) EQE-L curves and (c) EL spectra of BTrzICz, BTrzBCz and 4CzIPN with 20 wt% doping concentration

Reference

1. D. P. K. Tsang, T. Matsushima, C. Adachi, Sci. Rep. 2016, 6, 22463.
2. Im, W. Song, J. Y. Lee, J. Mater. Chem. C 2015, 3, 8061.